








Article

# Variation of the Chemical Composition of Waste Cooking Oils upon Bentonite Filtration

Alberto Mannu <sup>1,2,\*</sup>, Gina Vlahopoulou <sup>1,2</sup>, Paolo Urgeghe <sup>3</sup>, Monica Ferro <sup>1</sup>,  
Alessandra Del Caro <sup>3</sup>, Alessandro Taras <sup>4</sup>, Sebastiano Garroni <sup>4</sup>, Jonathan P. Rourke <sup>5</sup>,  
Roberto Cabizza <sup>3</sup> and Giacomo L. Petretto <sup>3,4,\*</sup>

<sup>1</sup> Department of Chemistry, Materials and Chemical Engineering "G. Natta", Politecnico di Milano, Piazza L. da Vinci 32, 20133 Milano, Italy; gvchimica@gmail.com (G.V.); monica.ferro@polimi.it (M.F.)

<sup>2</sup> Leibniz-Institut für Katalyse e. V., Albert-Einstein-Straße 29, 18059 Rostock, Germany

<sup>3</sup> Dipartimento di Agraria, Università degli Studi di Sassari, Viale Italia, 39, 07100 Sassari, Italy; paolou@uniss.it (P.U.); delcaro@uniss.it (A.D.C.); rcabizza@uniss.it (R.C.)

<sup>4</sup> Department of Chemistry and Pharmacy, via Vienna 2, University of Sassari, 07100 Sassari, Italy; tarassales@gmail.com (A.T.); sgarroni@uniss.it (S.G.)

<sup>5</sup> School of Chemistry, Cardiff University, Park Place, Cardiff CF10 3AT, UK; rourkej1@cardiff.ac.uk

\* Correspondence: alberto.mannu@polimi.it (A.M.); g.petretto@uniss.it (G.L.P.); Tel.: +39-022-3993045 (A.M.); +39-079-229538 (G.L.P.)

Received: 16 May 2019; Accepted: 5 June 2019; Published: 10 June 2019



**Abstract:** The chemical composition and the color of samples of waste cooking oils (WCOs) were determined prior to and after filtration on two different pads of bentonite differing in particle size. The volatile fraction was monitored by headspace solid-phase microextraction (HS-SPME) coupled with gas-chromatography, while the variation of the composition of the main components was analyzed by <sup>1</sup>H NMR. Both techniques allowed the detection of some decomposition products, such as polymers, terpenes, and derivatives of the Maillard process. The analysis of the chemical composition prior to and after bentonite treatment revealed a tendency for the clays to retain specific chemical groups (such as carboxylic acids or double bonds), independent of their particle size. A pair comparison test was conducted in order to detect the sensory differences of the intensity of aroma between the WCO treated with the two different bentonites. In addition, characterization of the bentonite by means of powder X-ray diffraction (XRD) and thermogravimetric measurements (TG) was performed.

**Keywords:** waste cooking oil; nuclear magnetic resonance; headspace solid-phase microextraction; thermogravimetry; principal components analysis; X-ray diffraction

## 1. Introduction

Among the many methods of cooking food, deep-fat frying is perhaps the most exploited, both in domestic and commercial kitchens (e.g., fast food restaurants). Fried food became popular mainly for economic (speed of processing) and sensory (palatable taste) reasons and is currently thought to be the most consumed type of cooked food worldwide [1]. During the cooking process, the rich chemical composition of the food is subjected to many chemical and physical transformations promoted by the high temperature and by the exposure to air.

Since an oxidation process is involved in the production of volatile organic compounds (VOCs), the concentration of oxygen is directly related to their production [2]. The production of VOCs, and in particular of off-flavor compounds, is also affected by the number of frying cycles, which lower the smoking point value and the unsaturation level of fatty acids, increasing the degree of polymerization

and negatively affecting the characteristics of the oil. Most of the studies reported to date regarding cooking oils are focused on the consequences of the frying process on the food, and the variation of the chemical-physical properties of the oil is only discussed in terms of possible contamination of the cooked food [3,4]. As waste cooking oils (WCOs) are becoming popular as green raw materials for bio-lubricant production, it would be useful to gain some knowledge about their chemical composition and the effect upon it caused by recycling procedures, such as, for instance, treatment with clays.

In fact, during the past few years, interest in the composition of the edible oil at the end of its life cycle has grown exponentially as WCOs, previously considered a by-product of food production, have been revealed to be an important raw material for several industries [5,6]. The increasing quantities of WCOs produced worldwide, as well as the environmental risk associated with their uncontrolled dispersion, forced local governments towards the implementation of specific regulations for enhancing its safe recycling or disposal [7]. The availability of WCOs is impressive despite the fact that recycling is compulsory in several countries, only around 0.6 of the estimated 4 Mt of WCOs produced per year is currently collected in Europe, meaning that about 3.4 Mt of accessible cheap raw material are available per year [8]. Many ways of reutilization have been explored and nowadays WCOs find applications in bio-lubricant production [9,10], as an additive for animal feed [11,12], and as the basis for eco-friendly biodegradable solvents [13]. WCOs can even be used as energy sources, through direct burning [14–17] or as an ingredient for the biodiesel production [18,19]. Important applications have been found in the construction sector, for example as an additive for bitumen binders [20,21] or in environmental chemistry, such as mercury sorbent devices [22].

In Europe, WCOs are defined as “municipal wastes” by the European Waste Catalogue [23] and are collected through the urban waste systems or directly delivered by the final user to a recycling point. The main consequence of this procedure is the generation of a complex mixture composed of different kinds of exhausted vegetable oils, most of them previously employed for frying, with different origins and compositions. The general chemical profile of WCOs is mainly constituted of triacylglycerols, glycerols, free fatty acids (FFAs), and several polymerization compounds. Physically, WCOs appear as dark and viscous, with a low smoking point. Usually, recycling of WCOs is performed by distillation (as in the bio-diesel industry) or by a degumming process followed by a filtration on a porous material such as bentonite or cellulose (normally done by small local industry). We recently studied the optimization of an acidic degumming procedure applied to WCOs in order to obtain valuable raw materials for the bio-lubricants production [24] and the monitoring of the variation of some physical parameters of the exhausted vegetable oils subjected to filtration on a pad of bentonite [25]. With the aim of extending our research to the improvement of the current regeneration methods for the recycling of WCOs, herein we discuss the variation of the volatile fraction, the  $^1\text{H}$  NMR profile, and of the color of samples of WCOs treated with two bentonites differing in particle size. Furthermore, a discussion of the relationship between the physical composition of the bentonites employed and the result of the clarification process is reported, including an exhaustive characterization of the bentonite prior to and after filtration by means of X-ray diffraction (XRD) and thermal gravimetric analysis (TG). Finally, the outcomes of a sensory test performed on the samples considered in the present study are reported and presented as part of the general discussion.

## 2. Materials and Methods

### 2.1. Starting Materials

With the aim of simulating the operating conditions of recycling industries, several samples of frying oils of unknown origin were randomly collected from domestic suppliers in the geographic area of Sardinia (Italy) and mixed, obtaining the crude oil WCO. The crude waste oil samples did not contain any visible suspended solids.

Bentonite collected from the cave of S'Aliderru (Sardinia, Italy) was purchased from Clariant. The former bentonite was not subjected to any acidic or basic activation process.

## 2.2. Clarification Procedure

Often, even in industrial applications, the particle size of the clays is not considered an influential parameter. Nevertheless, this aspect can be relevant as the chemical and physical processes which regulate the clarification procedures can give different outcomes depending on the specific particle size. In order to verify this statement, the raw bentonite was sifted sequentially with two consecutive metallic sieves with hole sizes of 1.8 and 2.36 mm, obtaining the samples B1 (1.18 mm < Ø < 2.36 mm) and B2 (Ø < 1.18 mm). Filters were set up by filling a 50 mL cartridge with 30 g of B1 or B2, and 30 g aliquots of WCO were filtered under atmospheric pressure. Even if the amount of bentonite necessary for the clarification procedure can be reduced, no capacity tests were performed, as the aim of the present study was to study the variation of the chemical composition of WCOs in optimal conditions.

The filtered materials were collected, giving WCO1 (filtered on B1) and WCO2 (filtered on B2). The filtrations were reproduced in triplicate and performed at room temperature.

## 2.3. Gas Chromatography–Mass Spectrometry (GC-MS) Analysis

The gas chromatography–mass spectrometry (GC-MS) analysis was carried out using an Agilent 7890 GC equipped with a Gerstel MPS autosampler, coupled with an Agilent 7000C MSD detector. The chromatographic separation was performed on a VF-Wax 60 m × 0.25 mm i.d., 0.5 µm film thickness column (Agilent). The following temperature program was used: 40 °C hold for 4 min, increased to 150 °C at a rate of 5.0 °C/min, hold for 3 min, then increased to 240 °C at a rate of 10 °C/min, and finally held for 12 min. Helium was used as the carrier gas at a constant flow of 1 mL/min. The data was analyzed using a MassHunter Workstation B.06.00 SP1, with identification of the individual components (Table 1) performed by comparison with the co-injected pure compounds and by matching the mass spectrometry (MS) fragmentation patterns and retention indices with the built-in library or literature data or commercial mass spectral libraries (NIST/EPA/NIH 2008; HP1607 purchased from Agilent Technologies).

### 2.3.1. Retention Indices

A hydrocarbon mixture of n-alkanes (C9-C22) was analyzed separately under the same chromatographic conditions described in the GC-MS section to calculate the retention indices with the generalized equation by Van del Dool et al. [26] (Equation (1)).

$$I_x = 100[(t_x - t_n)/(t_{n+1} - t_n) + n] \quad (1)$$

In Equation (1),  $t$  is the retention time,  $x$  is the analyte,  $n$  is the number of carbons of alkane that elute before the analyte, and  $n + 1$  is the number of carbons of alkane that elute after the analyte.

### 2.3.2. Headspace Solid-Phase Microextraction (HS-SPME)

A 100 µm polydimethylsiloxane/divinylbenzene/carboxen (PDMS/DVB/CAR)-coated fiber 50/30 Stableflex (Supelco, Sigma Aldrich, St. Louis, MO, USA) was preconditioned prior to use at 270 °C for 1 h in a Gerstel MPS bake-out station, according to the manufacturer's instructions. Then 5 g of sample were placed in a 20 mL SPME vial, 75.5 × 22.5 mm, that was tightly closed with a septum and allowed to equilibrate for 5 min at 60 °C. The preconditioned fiber was then exposed to the headspace. The extraction time was fixed at 30 min. All experiments were carried out under constant agitation at 250 rpm. After the extraction, the fiber was desorbed for 2 min into a Gerstel CIS6 PTV injector operating at 250 °C in a splitless injection mode. Results were reported as absolute peak area (×10<sup>6</sup>).

## 2.4. NMR Analysis

WCO samples were analyzed in pure form, using a coaxial tube with deuterated DMSO for a lock. <sup>1</sup>H NMR spectra were recorded on a Bruker AV500 spectrometer operating at 500 MHz for the proton

nucleus. All the experiments were performed at 305 K with the following acquisition parameters: time domain 32 K, relaxation delay 3 s, 128 scans, and a spectral width of 12 ppm, acquisition time 2.53 s.

#### 2.4.1. Determination of Hunter Lab Coordinates

Color measurements were carried out using a Minolta colorimeter (Minolta CR-300, Konica Minolta Sensing, Osaka, Japan), and the results were expressed in accordance to the Hunter Lab color space [27]. According to this methodology, the color space is organized in a cubic form where the descriptors are  $L^*$ ,  $a^*$ , and  $b^*$ . Parameters determined were  $L^*$  ( $L = 0$  (black) and  $L = 100$  (white)),  $a^*$  ( $-a =$  greenness and  $+a =$  redness),  $b^*$  ( $-b =$  blueness and  $+b =$  yellowness), and  $\Delta E$ -total color difference, as previously reported by Conte et al. [28]. The analyses were performed without any dilution. For samples comparison, the values of  $\Delta L^*$ ,  $\Delta a^*$ , and  $\Delta b^*$  indicate how much the samples differ from each other (e.g., if  $\Delta a$  increases from sample A to B, it means that A is greener than B).

#### 2.4.2. Sensory Evaluation

A paired comparison test was employed to determine the difference between the two samples of WCOs with regard the intensity of oil aroma. A panel composed of 45 consumers was asked to sniff the two oil samples treated with the two different bentonites (B1 and B2). The oil samples were presented to the assessors in a balanced and randomized order and labelled with a three-digit code. The sensory difference between the untreated WCO and the samples filtered on bentonite was so high that it was unnecessary to perform a sensory test to distinguish the untreated WCO from the filtered samples.

#### 2.5. Statistical Analysis

The multivariate analysis of WCO samples was carried out by subjecting the HS-SPME-GC data to a principal component analysis (PCA). The VOCs data of three samples of each WCO were used to define a  $m \times n$  matrix where  $m$  is the samples and  $n$  is the variables. The data were centered and autoscaled before the PCA. All PCA analyses were performed with an R-based chemometric software designed by Chemometric group of Chemical Italian Society [29]. All experiments were repeated three times ( $n = 3$ ). All statistical analyses were performed subjecting volatiles of WCOs samples to a one-way analysis of variance (ANOVA) when the data followed a normal distribution, using SigmaStat v 3.5 software. The distribution of the sample was evaluated by the Kolmogorov–Smirnov and Shapiro tests. A value of  $p < 0.05$  was considered statistically significant.

Sensory data were analyzed using the statistical table for paired comparison and paired difference test (two-tailed). The significance level of the test chosen was 5%.

#### 2.6. Thermogravimetric Analysis

The thermal stability of the bentonite was evaluated using a thermogravimetric apparatus (TGA) coupled with a differential scanning calorimeter (DSC) (Labsys Setaram). The experiment was carried out on 50–60 mg of sample under an Ar flow of  $120 \text{ mL min}^{-1}$ , between 25 and  $1000 \text{ }^\circ\text{C}$  using a heating and cooling rate of  $5 \text{ }^\circ\text{C min}^{-1}$  and  $30 \text{ }^\circ\text{C min}^{-1}$ , respectively. Alumina crucibles were used for the analysis in order to avoid undesired reactions with the powders during the annealing.

#### 2.7. XRD

X-ray diffraction (XRD) patterns of the bentonite samples were acquired with a Rigaku SmartLab powder diffractometer, operating in Bragg–Brentano geometry, equipped with a Cu-rotating anode X-ray source ( $K\alpha$ ,  $\lambda = 1.5418 \text{ \AA}$ ) and a graphite monochromator mounted on the diffracted beam. The powders were dispersed and compacted into an amorphous glass sample holder and the measurements recorded in the angular range of  $5\text{--}50 \text{ } 2\theta$  with a scan step of  $0.05^\circ$  per 4 s.

**Table 1.** Main VOCs detected, tentatively identified, by HS-SPME GC/MS analysis of WCO, WCO1, and WCO2. The values expressed are the result of the average value of three independent replicates  $\pm$  SD of absolute total ion chromatogram (TIC) peak area (1E6). PCA: symbols used for principal component analysis, V: variable, RT: retention time, RI: experimental retention index on a WF-WAX column, RI literature: retention index from NIST database,  $\Delta$  represents the difference between the experimental RI and the literature RI, n.d.: not detected, n.a.: not available (\*:  $p < 0.05$ ; \*\*:  $p < 0.01$ ).

PCA	RT	WCO	SD	WCO1	SD	WCO2	SD	RI	RI Literature	$\Delta$	Compound
V1	5.444	0.42	0.08	0.72 *	0.14	0.96	0.08	702	700	2	heptane
V2	5.573	0.89	0.03	0.28 **	0.13	0.11	0.01	711	702	9	acetaldehyde
V3	6.13	0.53	0.07	0.10 **	0.07	0.13	0.02	748	n.a.		Methylamine, N,N-dimethyl-
V4	6.881	1.12	0.26	2.22 *	0.72	3.46	0.53	799	800	1	octane
V5	9.65	0.20	0.04	0.10 *	0.01	0.05	0.00	910	907	3	2-Butanone
V6	10.132	0.72	0.39	0.48	0.28	0.43	0.10	925	918	7	Butanal, 3-methyl-
V7	10.579	0.14	0.00	n.d.		n.d.		939	971	32	Butyl-cyclopentane
V8	12.109	1.00	0.19	1.18	0.28	1.54	0.33	988	979	9	pentanal
V9	15.527	4.43	0.87	6.79	1.33	7.42	0.84	1091	1083	8	hexanal
V10	18.842	0.26	0.03	0.47	0.22	0.53	0.01	1193	1182	11	2-Heptanone
V11	18.94	0.31	0.24	0.86	0.08	1.19	0.50	1196	1184	12	Heptanal
V12	19.133	0.28	0.12	0.07 *	0.01	n.d.		1202	1185	17	Pyridine
V13	19.404	0.23	0.09	0.42 *	0.02	0.56	0.04	1211	1200	11	Limonene
V14	19.997	0.42	0.20	0.06 *	0.03	n.d.		1230	1212	18	Pyrazine
V15	20.184	0.50	0.14	0.24 *	0.09	n.d.		1237	1216	21	2-Hexenal, (E)-
V16	20.297	0.44	0.15	0.66	0.18	1.00	0.06	1240	1231	9	Furan, 2-pentyl-
V17	20.675	0.56	0.21	0.66	0.06	0.53	0.09	1253	1250	3	1-Pentanol
V18	20.884	0.48	0.17	0.56	0.02	0.70	0.09	1260	1246	14	$\gamma$ -terpinene
V19	21.500	0.20	0.15	n.d.		n.d.		1280	1272	8	Hexyl acetate
V20	21.728	0.81	0.15	0.06 **	0.02	0.03	0.01	1287	1266	21	Pyrazine, methyl-
V21	22.061	0.12	0.02	0.12	0.02	0.05	0.01	1298	1287	11	2-Octanone
V22	22.199	1.11	0.28	1.46	0.51	0.98	0.80	1303	1289	14	Octanal
V23	22.841	1.16	0.25	0.20 **	0.06	n.d.		1325	1303	22	2-Propanone, 1-hydroxy-
V24	23.448	2.09	0.44	2.28	0.24	1.87	0.53	1346	1322	24	2-Heptenal
V25	23.632	0.27	0.09	0.43	0.10	0.26	0.05	1353	1338	15	5-Hepten-2-one, 6-methyl-
V26	23.821	0.81	0.08	0.10 **	0.01	n.d.		1360	1326	34	Formamide, N,N-dimethyl-
V27	25.27	5.07	1.10	6.42	0.40	6.59	0.25	1410	1391	19	Nonanal
V28	26.032	1.25	0.25	0.23 **	0.08	0.38	0.00	1437	1414	23	N,N-Dimethylacetamide
V29	26.305	0.22	0.08	0.19	0.04	0.12	0.02	1447	1441	6	Ethyl octanoate
V30	26.463	0.79	0.08	0.69	0.04	0.56	0.20	1453	1429	24	2-Octenal, (E)-

Table 1. Cont.

PCA	RT	WCO	SD	WCO1	SD	WCO2	SD	RI	RI Literature	$\Delta$	Compound
V31	26.616	0.24	0.06	0.30	0.05	0.46	0.10	1458	1453	5	Heptanol
V32	26.756	11.05	0.74	n.d.		n.d.		1463	1449	14	Acetic acid
V33	27.498	12.72	1.03	3.64 **	1.69	0.17 *	0.19	1489	1461	28	Furfural
V34	28.121	0.97	0.20	n.d.		0.10	0.10	1511	n.a.		Pyridine, 4-ethenyl-
V35	28.554	0.64	0.06	0.32 **	0.06	0.12	0.03	1525	1495	30	2,4-Heptadienal,
V36	29.538	0.52	0.03	n.d.		n.d.		1557	1535	22	Propanoic acid
V37	29.787	1.90	0.38	1.66	0.13	2.00	0.40	1565	1534	31	2-Nonenal,
V38	31.011	1.32	0.04	0.38 **	0.23	0.08	0.01	1607	1570	37	2-Furancarboxaldehyde, 5-methyl-
V39	31.951	0.36	0.10	n.d.		n.d.		1646	1625	21	Butanoic acid
V40	32.627	2.00	0.14	1.75	0.24	1.07 *	0.17	1674	1644	30	2-Decenal, (E)-
V41	32.695	1.21	0.15	0.33 **	0.19	n.d.		1677	1660	17	Furanmethanol
V42	34.497	2.27	0.11	2.09	0.13	1.66 *	0.13	1764	1746	18	$\alpha$ -Farnesene
V43	34.857	1.06	0.07	0.72 **	0.02	0.35	0.07	1782	1752	30	2-Undecenal
V44	35.117	1.01	0.05	0.77 **	0.05	0.29	0.09	1795	1797	2	2,4-Decadienal, isomer 1
V45	35.997	4.48	0.02	2.76 **	0.45	0.39	0.20	1847	1811	36	2,4-Decadienal, isomer 2
V46	36.215	1.91	0.17	n.d.		n.d.		1860	1846	14	Hexanoic acid

### 3. Results and Discussion

#### 3.1. Characterization of the Volatile Organic Compounds (VOCs)

The intense smell typical of WCOs is related to the chemical composition, in particular to the volatile fraction. The VOCs of our samples were extracted by solid-phase microextraction (SPME) and analyzed by gas-chromatography coupled with mass spectrometry. Forty-six components were identified (Table 1).

As shown in Table 1, several classes of compounds were detected: aldehydes, alcohols, ketones, hydrocarbons, and acids.

Many of the decomposition compounds detected originate from the oxidation of triacylglycerols and from the Maillard process, which consists of the formation of nitrogen-containing derivatives as a consequence of a reaction between a carbonyl unit of a carbohydrate and an amino function of a protein. The presence of some terpenes is linked to the leaching from the fried food [1]. Taking into account that commercial vegetable oil is almost odorless; the chemicals responsible for the aroma of the fried oil must be produced during the frying process. The volatile compounds are strongly related to the perceived food quality, as the aroma is one of the most important factors in cooked food. Prolonged use of frying oil can cause these compounds to impart unpleasant flavors to food and can limit the re-utilization of the oil. Previous authors have reviewed the complex chemical processes involving the vegetable oil during frying, and, among others, the main reactions involved in the production of low molecular weight volatile compounds are the Maillard reaction, thermo-oxidation, and hydrolysis [30]. In particular, a consistent reduction of the odor in treated samples is related to the removing of acetic, propanoic, butanoic, and hexanoic acids and hexyl acetate.

Alkane compounds such as n-heptane, n-octane, butyl-cyclopentane have been detected and reported to be products of pyrolysis of vegetable oils [31]. Although some terpenes, such as camphene and limonene, were reported to be the result of heating treatment in peanut oil [32], isoprene derivatives found in our samples probably arose from spices used as flavoring agents during the frying. Furan derivatives, pyrazines, and, in general, nitrogen heterocycles, such as furan, 2-pentyl-pyridine-ethenyl, or 5-HMF, are a result of the Maillard reaction between food components.

Other chemicals deriving from the autoxidation of linoleic acid, which is one of the main precursors of aroma components in fried food, such as dienals (2,4-heptadienal or 2,4-decadienal), and alkenals, such as 2-undecenal, 2-decenal, and 2-octenal, were also detected [33].

Chromatographic analysis was carried out on raw samples as well as in samples filtered on a cartridge of bentonite (samples WCO1 and WCO2), and the results were expressed as absolute peak area ( $\times 10^6$ ) obtained by total ion current (TIC) chromatogram. In accordance with the results of Takeoka and coworkers, who analyzed WCOs of different origin [34], the major compounds detected in our samples were hexanal, furan, 2-pentyl, 2-heptanal, nonanal, acetic acid, furfural, 2-nonenal, 5-HMF, 2-decenal, furan methanol, 2,4-decadienal, and hexanoic acid. The comparison between crude and filtered samples reveals an important role of the bentonite in reducing the amount of several chemicals contained in the crude waste. As expected, reducing the particle size of the filter caused a larger amount of chemicals to be retained. Further, the GC analysis revealed that the bentonite is sensitive to the specific functional groups: organic acids (such as acetic or hexanoic acid) were almost completely retained, molecules with double bonds were partially retained, and some other compounds (e.g., alkanals) were not retained by the clay at all. Some compounds, like n-heptane or hexanal, were slightly increased after bentonite filtration. These differences are related to the different competition phenomena to which the compounds are subjected during the fiber extraction. SPME is commonly affected by both saturation and competition events [35], and the different concentration of the analytes in the headspace of crude and filtered oils could affect the relative area of compounds, which may be slightly increased with respect to the relative percentage area.

### 3.2. Principal Component Analysis

The data related to the VOCs content were subjected to a principal component analysis in order to identify any discrimination between the filtered samples and the control (raw WCOs). The data were centered and autoscaled, and then PCA was performed. The cumulative explained variance by the two first principal components was about 78% and, as reported in the score plot (Figure 1), the three samples were perfectly clustered in three different groups meaning that the information contained in the variables was suitable to discriminate the samples.

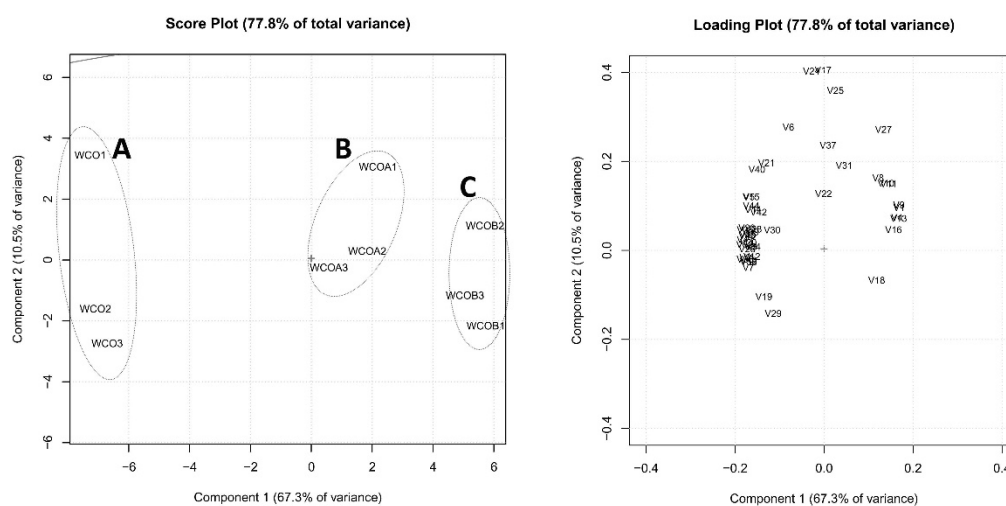


**Figure 1.** Score plot (left) and loading plot (right). A: WCO; B: WCO1; C: WCO2.

The main differentiation between the three groups (raw and filtered samples) occurs in the PC1, while on the PC2 a discrimination among the replicates is found. In the loading plot the variables are reported according to their contribution to the discrimination. The variables which contribute most to the discrimination along the first principal component are those located in the highest absolute values, namely: V20, 23, 26, 32, 33, 35, 36, 38, 39, 41, 43, 44, 46 (pyrazine, methyl-, 2-propanone, 1-hydroxy-, formamide, N,N-dimethyl-, acetic acid, furfural, 2,4-heptadienal, propanoic acid, 12-furancarboxaldehyde, 5-methyl-, butanoic acid, furanmethanol, 2-undecenal, 2,4-decadienal, hexanoic acid), which, as expected, are representative of organic acids and molecules which contain double bonds. Both classes of compounds are retained, or partially retained, by bentonite.

### 3.3. NMR

$^1\text{H}$  NMR has already been employed for the monitoring of oil deterioration processes during frying [36–38] and in a specific way for fatty acids determination [39,40]. This technique has some advantages with respect to the usual chromatographic methods, as it allows fast analysis, small sample volumes, and the simultaneous determination of multiple compounds [41]. In addition, Vigili [42] and Mannina [43] have employed NMR to identify the geographical origin of samples of olive oil.

Samples of crude cooking oil (WCO) and of the filtered WCO2 were analyzed by  $^1\text{H}$  NMR. The  $^1\text{H}$  NMR spectra show typical signals due to the fatty acids present in vegetable oils:  $-\text{CH}_3$  signals are located at 0.9 ppm; the  $\text{CH}_2$  fragment contained in the acyl chains can be found at 1.3, 1.6, and 2.3 ppm; while the methylenic signals of the unsaturated fatty acids, linolenyl acid, and glycerol lie at 2.0, 2.2, and between 4.0 and 4.4 ppm, respectively. Finally, the  $\text{CH-OCO-R}$  fragment of the triacylglycerols and the  $-\text{CH}=\text{CH}-$  moiety of the unsaturated fatty acids can be detected at 5.2 and 5.3 ppm (Figure 2). The pattern observed in WCO does not change after filtration on bentonite B2.



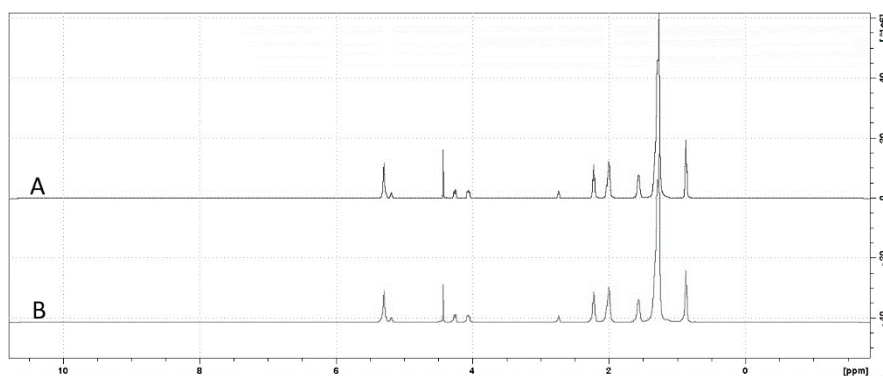


**Figure 2.** Comparison  $^1\text{H}$  NMR between crude (WCO) (A) and filtered samples (WCO2) (B).

From the  $^1\text{H}$  NMR data, it is possible to determine the fatty acid profile, according to the literature validated methodology of Popescu [44] (Table 2).

**Table 2.** Main components detectable at  $^1\text{H}$  NMR.

Analyte	Prior to Filtration (WCO)	After Filtration (WCO2)
Linolenic acid	<3%	<3%
Linoleic acid	13%	10%
Oleic acid	70%	70%
SFA <sup>a</sup>	16%	16%
IV <sup>b</sup>	83.2	83.8

<sup>a</sup> SFA = Saturated Fatty Acids. <sup>b</sup> Global unsaturation.

The data reported in Table 2 and the spectra shown in Figure 2 indicate that there is no significant difference in the amounts of the main fatty acids in the two samples and that the filtration on bentonite does not affect this aspect of the composition of WCO and WCO2. Minor products derived from the frying process (such as polymers, esters, and aldehydes) could also be detected by NMR. Treatment with bentonite resulted in the retention of some minor compounds (such as alkenals and alkadienals), as previously observed by GC analysis (Figure 3). In addition, no changes have been observed for the global unsaturation parameter, meaning that the ratio between linoleic and oleic acids is the same prior to and after filtration.

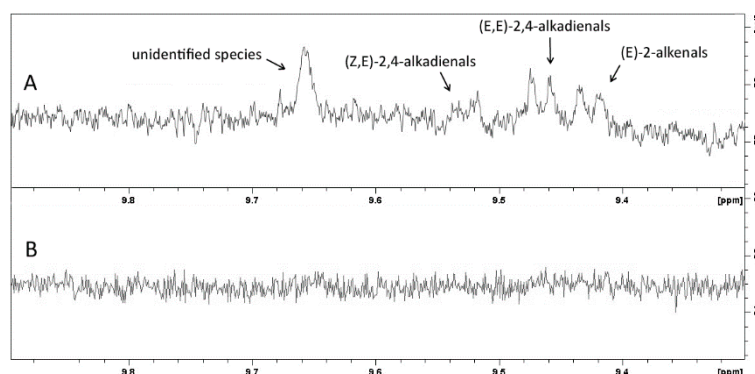


**Figure 3.** Comparison  $^1\text{H}$  NMR (aldehydes portion of the spectra) between crude (WCO) (A) and filtered samples (WCO2) (B).

### 3.4. Color

The WCOs appear as deep dark-brown oils with the color normally associated with the presence of oxidation products, polymers [45], traces of metals, and derivatives of the Maillard reaction [34].

Color measurements were conducted on samples of crude WCO (WCO), and on both filtered samples (WCO1 and WCO2) (Table 3).

**Table 3.** Color coordinates for crude and filtered samples of WCOs. <sup>a</sup> Commission Internationale de l’Eclairage; <sup>b</sup> The values reported were calculated as results of four measurements; the standard deviation is indicated. <sup>c</sup> L, lightness; <sup>d</sup> a, green–red; <sup>e</sup> b, blue–yellow; <sup>e</sup> E: total color difference.

Entry	Sample	Color (CIE) <sup>a</sup> (S) <sup>b</sup>			
		L <sup>c</sup>	a <sup>d</sup>	b <sup>e</sup>	$\Delta E$ ( $\Delta S$ )
1	WCO	23.11 (0.02)	3.25 (0.05)	9.33 (0.04)	
2	WCO1	25.22 (0.02)	2.19 (0.10)	12.62 (0.05)	4.04 (0.06)
3	WCO2	27.17 (0.01)	0.21 (0.05)	15.25 (0.05)	7.79 (0.05)

From the data in Table 3, we can observe that the treatment with bentonite considerably changed the color characteristics of the oils. Filtered samples show increased values of lightness (L), a lowering of the red, and an increase of the yellow components (respectively, lower values of a and higher values of b; entry 1 versus entries 2 and 3) compared with the crude samples. The overall visual change of the samples after clarification was from dark brown (WCO) to light yellow.

Some differences can be observed between the two different filtered samples (entry 1 versus entry 2): samples filtered with smaller-grain bentonite (WCO2) gave a more transparent oil, compared with samples treated with coarse-grain bentonite. The value of the total color difference  $\Delta E$  ( $E > 3$ , entries 2 and 3) indicates a significant change in color after filtration, perceptible to the human eye for both samples [46].

### 3.5. Sensory Evaluation

The total number of times each oil sample was selected by assessors as the most intensely smelling was determined. The data collected did not suggest a significant difference ( $p < 0.05$ ) between the two filtered oils, even if the panel of consumers showed a slight tendency to perceive the oil WCO1 as having the more intense odor, compared with WCO2 (26 responses versus 19). The sensory difference among the crude samples prior to filtration and the two filtered oils was so high that it was unnecessary to perform a blind test. Considering the waste classification of used oils and the fact that re-utilization in the food industry is forbidden, no other sensory tests involving taste or touch were performed.

### 3.6. Characterization of Bentonite

Clays and in particular bentonites are commonly used as blanching agents in the vegetable oil production, as they can remove chlorophylls, phospholipids, lectines, metals, and oxidation products [47,48]. Bentonite is a porous material characterized by a large available surface area, which is responsible for both chemical and physical interactions with the oil components that are retained (bleaching capacity) [49].

Combining the results obtained through the above-described methodologies, we see that the treatment of WCOs with bentonite is effective mainly at removing some polar compounds, particularly those with acidic groups or with multiple-bonds. This removal of conjugated compounds, combined with the retention of metal particles and some cations, produces an enhancement of the lightness in the filtered samples. In order to relate these findings to the physical characteristics of the bentonite employed, we studied samples of bentonite prior to and after filtration by powder X-ray diffraction (XRD) and thermogravimetry (TG). The exhausted bentonite considered was that with the smaller grain size (B2), as it had been shown to retain more of the contaminants.

Bentonite is known for its purity with a high content of montmorillonite and the presence of quartz, mostly in respirable size [50]. XRD analysis confirmed this: montmorillonite, cristobalite, and quartz were observed as major phases in all of the samples (Figure 4).

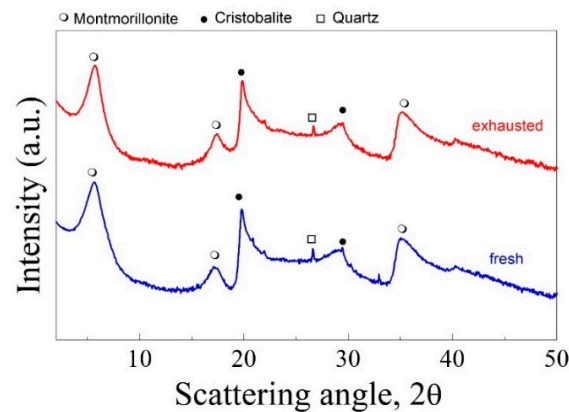


Figure 4. XRD profile of samples of fresh and exhausted bentonite.

From Figure 4, it is also possible to observe that no changes to the physical composition occurred during the filtration procedure: the phases present in the fresh sample, are still observed in the post-filtration sample; furthermore, each phase has a similar microstructure. However, the montmorillonite peak at  $5\ 2\theta$  is shifted to lower angles, suggesting a swelling of the clay layers, in accordance with the presence of residual materials in the pores after filtration.

### 3.7. Thermogravimetric Studies

The thermal stability of the “fresh” bentonite and the B2 material after filtration was evaluated by thermogravimetric analysis (TG, Figure 5).

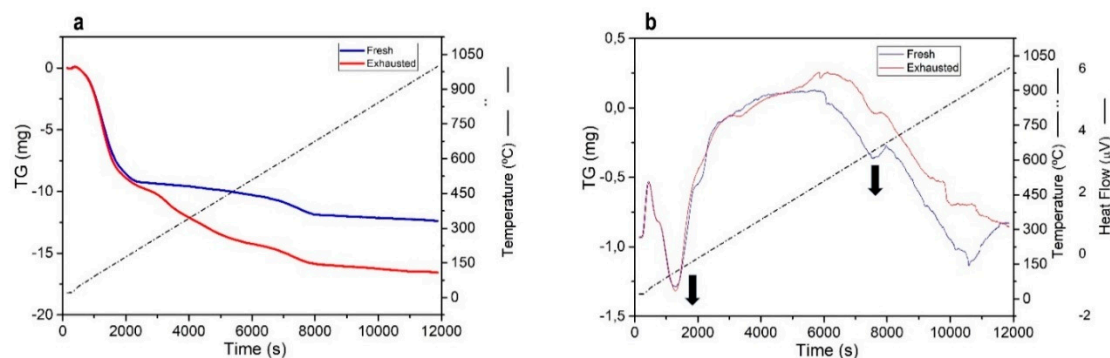


Figure 5. (a) Thermogravimetry profiles of fresh (blue line) and exhausted (red line) bentonites and (b) heat flow plot of fresh (blue line) and exhausted (red line) bentonites. The dotted line represents the temperature profile (°C).

The TG profile (Figure 5, left) shows two main endothermic peaks indicative of mass loss related to the elimination of water for both samples. One, between 60 and 150 °C, corresponding to the 15% of the total initial mass, can be referred to the physically adsorbed water, which is lost in an amount of 9.23 mg. The second event, between 600 and 750 °C, can be related to the condensation of the oxidryl structure, expulsed in the form of water [51]. Similar results have been observed in the case of Brazilian [52] and Turkish [53] bentonites. Even though a similar loss of water is recorded in both of our samples in the temperature range 60–150 °C, a clear difference can be observed for the two systems at higher temperatures. This difference, roughly 7 mg (200–1000 °C), can be ascribed to the quantity of residue adsorbed into the pores of the bentonites during the filtration treatment, further confirming the benefit of filtration. The DSC profile (Figure 4, right) shows a clear endothermic event peak at 105 °C. Other thermal events were also observed at higher temperatures: 600 °C (fresh and exhausted samples) and 810 °C (exhausted sample). Even though these events could be associated with the condensation

of the oxidryl groups and with the decomposition of the adsorbed residues, a proper determination needs further efforts in terms of characterization and will be addressed in a future work.

#### 4. Conclusions

The effect of the bentonite filtration of waste cooking oils (WCOs) on their chemical composition was evaluated by headspace solid-phase microextraction (HS-SPME) coupled with gas-chromatography and <sup>1</sup>H NMR for the first time. The filtration process represents an important step in the industrial recycling of this by-product of food preparation for non-bio-diesel applications. The analysis of the volatile fractions revealed the ability of the bentonite to retain compounds containing specific chemical groups. In particular, organic acids were almost completely retained, molecules containing double bonds were partially retained, and other groups, like alkanes or alkanals, were not retained by the clay.

Experiments conducted on bentonites of different grain sizes showed that it is possible to enhance the amount of chemicals retained by only reducing the size of the bentonite particles. The data acquired suggest that even a change in the grain size of the clay can affect the clarification procedure. This aspect should be considered carefully when bentonites are employed for the recycling of waste cooking oils. Some of the techniques herein presented, such as the headspace solid-phase microextraction (HS-SPME) coupled with gas-chromatography or the Hunter Lab color determination, could represent useful tools for monitoring the saturation levels of industrial bentonites.

The treatment with bentonite also positively affected the color of WCO as confirmed by the spectrophotometric analysis; although this change was also perceptible to the naked human eye.

Finally, thermogravimetric analysis and XRD measurements on the bentonite prior to and after oil treatment suggest no changes to the bentonite functionalities as a result of WCO filtration.

**Author Contributions:** Methodology and investigation: A.M. and G.V.; GC-MS and color analysis: G.L.P.; NMR investigation: M.F.; sensory evaluation: A.D.C.; characterizations on bentonites: A.T.; data curation: P.U. and S.G.; Awriting—original draft preparation: A.M. and G.L.P.; writing—review and editing: J.P.R. and R.C.; and funding acquisition: P.U.

**Funding:** This research received no external funding.

**Conflicts of Interest:** The authors declare no conflict of interest.

#### References

1. Choe, E.; Min, D.B. Chemistry of Deep-Fat Frying Oils. *J. Food Sci.* **2007**, *72*, R77–R86. [[CrossRef](#)] [[PubMed](#)]
2. Pokorny, J. Flavor chemistry of deep fat frying in oil. In *Flavor Chemistry of Lipid Foods*; Min, D.B., Smouse, T.H., Zhang, S.S., Eds.; American Oil Chemists Society: Champaign, IL, USA, 1989; p. 113.
3. Ziaifar, A.M.; Achir, N.; Courtois, F.; Trezzani, I.; Trystram, G. Review of mechanisms, conditions, and factors involved in the oil uptake phenomenon during the deep-fat frying process. *Int. J. Food Sci. Technol.* **2008**, *43*, 1410–1423. [[CrossRef](#)]
4. Saguy, I.; Dana, D. Integrated approach to deep fat frying: Engineering, nutrition, health and consumer aspects. *J. Food Eng.* **2003**, *56*, 143–152. [[CrossRef](#)]
5. Ramos, T.R.P.; Gomes, M.I.; Barbosa-Póvoa, A.P. Planning waste cooking oil collection systems. *Waste Manag.* **2013**, *33*, 1691–1703. [[CrossRef](#)] [[PubMed](#)]
6. Borrello, M.; Caracciolo, F.; Lombardi, A.; Pascucci, S.; Cembalo, L. Consumers' Perspective on Circular Economy Strategy for Reducing Food Waste. *Sustainability* **2017**, *9*, 141. [[CrossRef](#)]
7. Li, Y.; Jin, Y.; Li, J.; Chen, Y.; Gong, Y.; Li, Y.; Zhang, J. Current Situation and Development of Kitchen Waste Treatment in China. *Procedia Environ. Sci.* **2016**, *31*, 40–49. [[CrossRef](#)]
8. Eubia.org. Available online: <http://www.eubia.org/cms/wiki-biomass/biomass-resources/challenges-related-to-biomass/used-cooking-oil-recycling/> (accessed on 1 April 2019).
9. Petran, J.; Pedisic, L.; Orlovic, M.; Podolski, S.; Bradac, V. Biolubricants from natural waste oil and fats. *Goriva Maz.* **2008**, *47*, 463–478.
10. Shashidhara, Y.M.; Jayaram, S.R. Vegetable oils as a potential cutting fluid—An evolution. *Tribol. Int.* **2010**, *43*, 1073–1081. [[CrossRef](#)]

11. Salemdaab, R.; Zu Ermgassen, E.K.; Kim, M.H.; Balmford, A.; Al-Tabbaa, A. Environmental and health impacts of using food waste as animal feed: A comparative analysis of food waste management options. *J. Clean. Prod.* **2017**, *140*, 871–880. [[CrossRef](#)] [[PubMed](#)]
12. Tres, A.; Bou, R.; Guardiola, F.; Nuchi, C.D.; Magrinya, N.; Codony, R. Use of recovered frying oils in chicken and rabbit feeds: Effect on the fatty acid and tocol composition and on the oxidation levels of meat, liver and plasma. *Animal* **2013**, *7*, 505–517. [[CrossRef](#)] [[PubMed](#)]
13. Panadare, D.C.; Rathod, V.K. Applications of Waste Cooking Oil Other Than Biodiesel: A Review. *Iran. J. Chem. Eng.* **2015**, *12*, 55–76.
14. Singhabhandhu, A.; Tezuka, T. The waste-to-energy framework for integrated multi-waste utilization: Waste cooking oil, waste lubricating oil, and waste plastics. *Energy* **2010**, *35*, 2544–2551. [[CrossRef](#)]
15. Singhabhandhu, A.; Tezuka, T. Prospective framework for collection and exploitation of waste cooking oil as feedstock for energy conversion. *Energy* **2010**, *35*, 1839–1847. [[CrossRef](#)]
16. Namoco, C.S., Jr.; Comaling, V.C.; Buna, C.C., Jr. Utilization of used cooking oil as an alternative cooking fuel resource. *ARPJ. Eng. Appl. Sci.* **2017**, *12*, 435–442.
17. Capuano, D.; Costa, M.; Di Fraia, S.; Massarotti, N.; Vanoli, L. Direct use of waste vegetable oil in internal combustion engines. *Renew. Sustain. Energy Rev.* **2017**, *69*, 759–770. [[CrossRef](#)]
18. No, S.-Y. Inedible vegetable oils and their derivatives for alternative diesel fuels in CI engines: A review. *Renew. Sustain. Energy Rev.* **2011**, *15*, 131–149. [[CrossRef](#)]
19. Talebian-Kiakalaieh, A.; Amin, N.A.S.; Mazaheri, H. A review on novel processes of biodiesel production from waste cooking oil. *Appl. Energy* **2013**, *104*, 683–710.
20. Sun, D.; Lu, T.; Xiao, F.; Zhu, X.; Sun, G. Formulation and aging resistance of modified bio-asphalt containing high percentage of waste cooking oil residues. *J. Clean. Prod.* **2017**, *161*, 1203–1214. [[CrossRef](#)]
21. Asli, H.; Ahmadiania, E.; Zargar, M.; Karim, M.R. Investigation on physical properties of waste cooking oil – Rejuvenated bitumen binder. *Constr. Build. Mater.* **2012**, *37*, 398–405. [[CrossRef](#)]
22. Worthington, M.J.H.; Kucera, R.L.; Albuquerque, I.S.; Gibson, C.T.; Sibley, A.; Slattery, A.D.; Campbell, J.A.; Alboaiji, S.F.K.; Muller, K.A.; Young, J.; et al. Laying Waste to Mercury: Inexpensive Sorbents Made from Sulfur and Recycled Cooking Oils. *Chem. A Eur. J.* **2017**, *23*, 16219–16230. [[CrossRef](#)]
23. Waste Framework Directive. Available online: <http://ec.europa.eu/environment/waste/framework/list.htm> (accessed on 1 April 2019).
24. Vlahopoulou, G.; Petretto, G.L.; Garroni, S.; Piga, C.; Mannu, A. Variation of density and flash point in acid degummed waste cooking oil. *J. Food Process. Preserv.* **2018**, *42*, e13533. [[CrossRef](#)]
25. Mannu, A.; Vlahopoulou, G.; Sireus, V.; Petretto, G.L.; Mulas, G.; Garroni, S. Bentonite as a Refining Agent in Waste Cooking Oils Recycling: Flash Point, Density and Color Evaluation. *Nat. Prod. Commun.* **2018**, *13*, 613–616. [[CrossRef](#)]
26. Van Del Dool, H.; Kartz, P.D. A generalization of the retention index system including linear temperature programmed gas-liquid partition chromatography. *J. Chromatogr.* **1963**, *11*, 463–471. [[CrossRef](#)]
27. Petretto, G.L.; Tuberoso, C.I.G.; Vlahopoulou, G.; Atzei, A.; Mannu, A.; Zrira, S.; Pintore, G. Volatiles, color characteristics and other physico-chemical parameters of commercial Moroccan honeys. *Nat. Prod. Res.* **2016**, *30*, 286–292. [[CrossRef](#)] [[PubMed](#)]
28. Conte, P.; Del Caro, A.; Balestra, F.; Piga, A.; Fadda, C. Bee pollen as a functional ingredient in gluten-free bread: A physical-chemical, technological and sensory approach. *LWT Food Sci. Technol.* **2018**, *90*, 1–7. [[CrossRef](#)]
29. Gruppo di Chemiometria. Available online: <http://gruppochemiometria.it/index.php/software> (accessed on 1 March 2019).
30. Zhang, Q.; Liu, C.; Sun, Z.; Hu, X.; Shen, Q.; Wu, J. Authentication of edible vegetable oils adulterated with used frying oil by Fourier Transform Infrared Spectroscopy. *Food Chem.* **2012**, *132*, 1607–1613. [[CrossRef](#)] [[PubMed](#)]
31. Alencar, J.W.; Alves, P.B.; Craveiro, A.A. Pyrolysis of tropical vegetable oils. *J. Agric. Food Chem.* **1983**, *31*, 1268–1270. [[CrossRef](#)]
32. Chung, T.Y.; Eiserich, J.P.; Shibamoto, T. Volatile compounds identified in headspace samples of peanut oil heated under temperatures ranging from 50 to 200 °C. *J. Agric. Food Chem.* **1993**, *41*, 1467–1470. [[CrossRef](#)]
33. Wu, C.-M.; Chen, S.-Y. Volatile compounds in oils after deep frying or stir frying and subsequent storage. *J. Am. Oil Chem. Soc.* **1992**, *69*, 858–865. [[CrossRef](#)]

34. Takeoka, G.R.; Full, G.H.; Dao, L.T. Effect of Heating on the Characteristics and Chemical Composition of Selected Frying Oils and Fats. *J. Agric. Food Chem.* **1997**, *45*, 3244–3249. [[CrossRef](#)]
35. Urgeghe, P.; Piga, C.; Addis, M.; Di Salvo, R.; Piredda, G.; Scintu, M.F.; Wolf, I.V.; Sanna, G. SPME/GC-MS Characterization of the Volatile Fraction of an Italian PDO Sheep Cheese to Prevalent Lypolytic Ripening: The Case of Fiore Sardo. *Food Anal. Methods* **2012**, *5*, 723–730. [[CrossRef](#)]
36. Dais, P.; Spyros, A.; Christophoridou, S.; Hatzakis, E.; Fragaki, G.; Agiomyrgianaki, A.; Salivaras, E.; Siragakis, G.; Daskalaki, D.; Tasioula-Margari, M.; et al. Comparison of Analytical Methodologies Based on <sup>1</sup>H and <sup>31</sup>P NMR Spectroscopy with Conventional Methods of Analysis for the Determination of Some Olive Oil Constituents. *J. Agric. Food Chem.* **2007**, *55*, 577–584. [[CrossRef](#)] [[PubMed](#)]
37. Siciliano, C.; Belsito, E.; De Marco, R.; Di Gioia, M.L.; Leggio, A.; Liguori, A. Quantitative determination of fatty acid chain composition in pork meat products by high resolution <sup>1</sup>H NMR spectroscopy. *Food Chem.* **2013**, *136*, 546–554. [[CrossRef](#)] [[PubMed](#)]
38. Jiang, X.; Huang, R.; Wu, S.; Wang, Q.; Zhang, Z. Correlations between <sup>1</sup>H NMR and conventional methods for evaluating soybean oil deterioration during deep frying. *J. Food Meas. Charact.* **2018**, *12*, 1420–1426. [[CrossRef](#)]
39. Castejón, D.; Mateos-Aparicio, I.; Molero, M.D.; Cambero, M.I.; Herrera, A. Evaluation and Optimization of the Analysis of Fatty Acid Types in Edible Oils by <sup>1</sup>H-NMR. *Food Anal. Methods* **2014**, *6*, 1285–1297. [[CrossRef](#)]
40. Corsaro, C.; Mallamace, D.; Vasi, S.; Ferrantelli, V.; Dugo, G.; Cicero, N. <sup>1</sup>H HR-MAS NMR Spectroscopy and the Metabolite Determination of Typical Foods in Mediterranean Diet. *J. Anal. Methods Chem.* **2015**, *2015*, 1–14. [[CrossRef](#)] [[PubMed](#)]
41. Hatzakis, E.; Agiomyrgianaki, A.; Kostidis, S.; Dais, P. High-Resolution NMR Spectroscopy: An Alternative Fast Tool for Qualitative and Quantitative Analysis of Diacylglycerol (DAG) Oil. *J. Am. Oil Chem. Soc.* **2011**, *88*, 1695–1708. [[CrossRef](#)]
42. Vigli, G.; Philippidis, A.; Spyros, A.; Dais, P. Classification of Edible Oils by Employing <sup>31</sup>P and <sup>1</sup>H NMR Spectroscopy in Combination with Multivariate Statistical Analysis. A Proposal for the Detection of Seed Oil Adulteration in Virgin Olive Oils. *J. Agric. Food Chem.* **2003**, *51*, 5715–5722. [[CrossRef](#)]
43. Camin, F.; Pavone, A.; Bontempo, L.; Wehrens, R.; Paolini, M.; Faberi, A.; Marianella, R.M.; Capitani, D.; Vista, S.; Mannina, L. The use of IRMS, <sup>1</sup>H NMR and chemical analysis to characterise Italian and imported Tunisian olive oils. *Food Chem.* **2016**, *196*, 98–105. [[CrossRef](#)]
44. Popescu, R.; Costinel, D.; Dinca, O.R.; Marinescu, A.; Stefanescu, I.; Ionete, R.E. Discrimination of vegetable oils using NMR spectroscopy and chemometrics. *Food Control* **2015**, *48*, 84–90. [[CrossRef](#)]
45. Martínez-Yusta, A.; Guillen, M.D. A study by <sup>1</sup>H nuclear magnetic resonance of the influence on the frying medium composition of some soybean oil-food combinations in deep-frying. *Food Res. Int.* **2014**, *55*, 347–355. [[CrossRef](#)]
46. Collar, C.; Jiménez, T.; Conte, P.; Fadda, C. Impact of ancient cereals, pseudocereals and legumes on starch hydrolysis and antiradical activity of technologically viable blended breads. *Carbohydr. Polym.* **2014**, *113*, 149–158. [[CrossRef](#)] [[PubMed](#)]
47. Kheok, S.C.; Lim, E.E. Mechanism of palm oil bleaching by montmorillonite clay activated at various acid concentrations. *J. Am. Oil Chem. Soc.* **1982**, *59*, 129–131. [[CrossRef](#)]
48. Taylor, D.R.; Jenkins, D.B.; Ungermann, C.B. Bleaching with alternative layered minerals: A comparison with acid-activated montmorillonite for bleaching soybean oil. *J. Am. Oil Chem. Soc.* **1989**, *66*, 334–341. [[CrossRef](#)]
49. Makhoukhi, B.; Didi, M.A.; Villemin, D.; Azzouz, A. Acid activation of Bentonite for use as a vegetable oil bleaching agent. *Grasas y Aceites* **2009**, *60*, 343–349. [[CrossRef](#)]
50. Mannu, A.; Vlachopoulou, G.; Sireus, V.; Mulas, G.; Petretto, G.L. Characterization of Sardinian Bentonite. *J. Sci. Res.* **2019**, *11*, 145–150. [[CrossRef](#)]
51. Suchithra, P.; Vazhayal, L.; Mohamed, A.P.; Ananthakumar, S. Mesoporous organic–inorganic hybrid aerogels through ultrasonic assisted sol–gel intercalation of silica–PEG in bentonite for effective removal of dyes, volatile organic pollutants and petroleum products from aqueous solution. *Chem. Eng. J.* **2012**, *200*, 589–600. [[CrossRef](#)]

52. De Oliveira, C.I.R.; Rocha, M.C.G.; Da Silva, A.L.N.; Bertolino, L.C. Characterization of bentonite clays from Cubati, Paraíba (Northeast of Brazil). *Cerâmica* **2016**, *62*, 272–277. [[CrossRef](#)]
53. Caglar, B.; Afsin, B.; Tabák, Á.; Eren, E. Characterization of the cation-exchanged bentonites by XRPD, ATR, DTA/TG analyses and BET measurement. *Chem. Eng. J.* **2009**, *149*, 242–248. [[CrossRef](#)]



© 2019 by the authors. Licensee MDPI, Basel, Switzerland. This article is an open access article distributed under the terms and conditions of the Creative Commons Attribution (CC BY) license (<http://creativecommons.org/licenses/by/4.0/>).